AD-A162 320 X-RAY LINE RATIOS FOR FE XVII OBSERVED IN THE SOLAR CORONA(U) AEROSPACE CORP EL SEGUNDO CA SPACE SCIENCES LAB H R RUGGE ET AL. 02 DEC 85 TR-0086(6940-01)-1 1/1

UNCLASSIFIED SD-TR-85-86 F04701-85-C-0086 F/G 3/2 NL

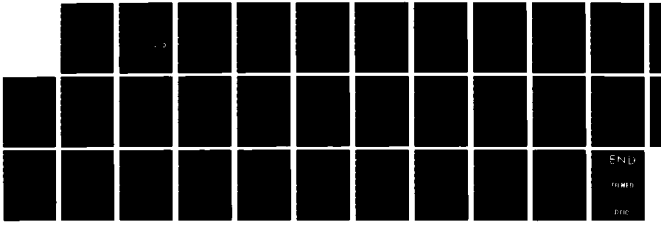

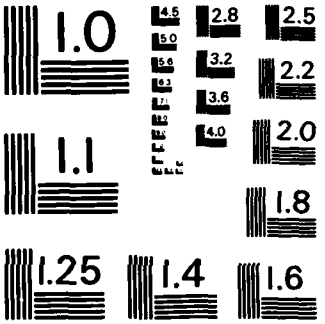

MICROCOPY RESOLUTION TEST CHART
NATIONAL BUREAU OF STANDARDS-1963-A

REPORT SD-TR-85-86

(2)

AD-A162 320

X-Ray Line Ratios for Fe XVII Observed in the Solar Corona

H. R. RUGGE and D. L. McKENZIE
Space Sciences Laboratory
Laboratory Operations
The Aerospace Corporation
El Segundo, CA 90245

2 December 1985

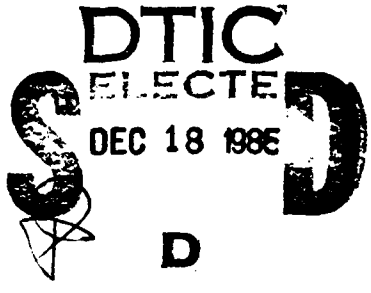

APPROVED FOR PUBLIC RELEASE;
DISTRIBUTION UNLIMITED

DTIC FILE COPY

Prepared for

SPACE DIVISION
AIR FORCE SYSTEMS COMMAND
Los Angeles Air Force Station
P.O. Box 92960, Worldway Postal Center
Los Angeles, CA 90009-2960

85 12 17 113

This report was submitted by The Aerospace Corporation, El Segundo, CA 90245, under Contract No. F04701-85-C-0086 with the Space Division, P.O. Box 92960, Worldway Postal Center, Los Angeles, CA 90009-2960. It was reviewed and approved for The Aerospace Corporation by G. A. Paulikas, Vice President, Laboratory Operations.

Maj Edmund D. Daszewski, SD/WE, was the project officer for the Mission-Oriented Investigation and Experimentation (MOIE) Program.

This report has been reviewed by the Public Affairs Office (PAS) and is releasable to the National Technical Information Service (NTIS). At NTIS, it will be available to the general public, including foreign nationals.

This technical report has been reviewed and is approved for publication. Publication of this report does not constitute Air Force approval of the report's findings or conclusions. It is published only for the exchange and stimulation of ideas.

Edmund D. Daszewski

EDMUND D. DASZEWSKI, Maj, USAF
MOIE Project Officer
SD/WE

Joseph Hess

JOSEPH HESS, GM-15
Director, AFSTC West Coast Office
AFSTC/WCO OL-AB

UNCLASSIFIED

SECURITY CLASSIFICATION OF THIS PAGE *(When Data Entered)*

REPORT DOCUMENTATION PAGE		READ INSTRUCTIONS BEFORE COMPLETING FORM
1. REPORT NUMBER SD-TR-85-86	2. GOVT ACCESSION NO. AD-A162 320	3. RECIPIENT'S CATALOG NUMBER
4. TITLE *(and Subtitle)* X-RAY LINE RATIOS FOR Fe XVII OBSERVED IN THE SOLAR CORONA		5. TYPE OF REPORT & PERIOD COVERED
		6. PERFORMING ORG. REPORT NUMBER TR-0086(6940-01)-1
7. AUTHOR(s) Hugo R. Rugge and David L. McKenzie		8. CONTRACT OR GRANT NUMBER(s) F04701-85-C-0086
9. PERFORMING ORGANIZATION NAME AND ADDRESS The Aerospace Corporation El Segundo, CA 90245		10. PROGRAM ELEMENT, PROJECT, TASK AREA & WORK UNIT NUMBERS
11. CONTROLLING OFFICE NAME AND ADDRESS Space Division Los Angeles Air Force Station Los Angeles, CA 90009-2960		12. REPORT DATE 2 December 1985
		13. NUMBER OF PAGES 32
14. MONITORING AGENCY NAME & ADDRESS*(if different from Controlling Office)*		15. SECURITY CLASS. *(of this report)* Unclassified
		15a. DECLASSIFICATION/DOWNGRADING SCHEDULE

16. DISTRIBUTION STATEMENT *(of this Report)*
Approved for public release; distribution unlimited..

17. DISTRIBUTION STATEMENT *(of the abstract entered in Block 20, if different from Report)*

18. SUPPLEMENTARY NOTES

19. KEY WORDS *(Continue on reverse side if necessary and identify by block number)*
Sun:corona
Sun:flares
Sun:spectra
X rays:spectra

20. ABSTRACT *(Continue on reverse side if necessary and identify by block number)*
Selected spectra from the SOLEX B X-ray spectrometers aboard the USAF P78-1 satellite ~~have been~~ analyzed in order to compare Fe XVII line flux ratios with theory. The spectra were chosen to cover a wide range of activity from quiescent active regions to large flares. For purposes of comparison with theory, a temperature scale based on a ratio of Fe XVIII to Fe XVII line fluxes has been derived. Fe XVII line ratios involving one line with a 3s

DD FORM 1473 (FACSIMILE)

UNCLASSIFIED

SECURITY CLASSIFICATION OF THIS PAGE *(When Data Entered)*

19. KEY WORDS (Continued)

20. ABSTRACT (Continued)

outer electron in the upper state and the other with a 3d electron are potentially the most useful, since such ratios are predicted, by theory, to have a significant temperature dependence. The data do not support the theoretical predictions. The dependence of the 3s/3d line ratios on temperature is found to be very weak, and the ratios are unlikely to be useful as temperature diagnostics. Measurements of the ratios involving only 3s upper levels or only 3d upper levels also disagree with theory. Improved theoretical calculations are needed to interpret the large amount of high-quality data that are now becoming available.

Simple calculations indicate that resonance scattering in the corona can have a significant effect on the observed $2p^6\ {}^1S_0 - 2p^5 3d\ {}^1P_1$ line flux, and observations verify this prediction. The effect of resonance scattering depends on the detailed geometry of the coronal regions in which the radiation is emitted and through which it propagates. This dependence can account for our observations of relatively large variances in line ratios involving the $3d\ {}^1P_1$ line.

CONTENTS

FIGURES

I. INTRODUCTION

The X-ray lines of neon-like iron, Fe XVII, are among the most intense emitted in the solar corona, both during and in the absence of flares. Among the strong Fe X-ray lines, these are emitted at the lowest coronal temperature, and they are the strongest (McKenzie et al. 1980). Only the n=2-1 transitions of O VII and O VIII are comparable in intensity to the strongest Fe XVII lines in the corona. The Fe XVII lines are principally valuable as temperature diagnostics in flares or active regions. They are not emitted at the low temperatures that prevail in the quiet corona outside active regions.

In this report we discuss a large number of observations of Fe XVII spectra from both active regions and flares. The 53 spectra used in this study were selected to cover as wide a range of solar activity as possible. For a given Fe XVII line, the measured flux ranged over a factor of more than 50, and that for the Fe XVIII emission at 14.20 Å varied by nearly a factor of 800. All of the spectra used were obtained in 1979 or 1980. Fe XVII line ratios deduced from these data are compared with recent calculations by Smith et al. (1984, hereafter SRMC) and with the earlier work of Loulergue and Nussbaumer (1973; 1975, hereafter LN). A number of nonflare Fe XVII spectra with moderate to high spectral resolution have been taken with rocket- or satellite-borne spectrometers (e.g., Parkinson 1973, 1975; Walker, Rugge, and Weiss 1974;

Hutcheon, Pye, and Evans 1976), and a few flare observations have been reported (McKenzie et al. 1980; Phillips et al. 1982). Here we will discuss 53 spectra measured by the SOLEX B RAP (rubidium acid phthalate) crystal spectrometer aboard the USAF P78-1 satellite. We treat flux ratios involving only the five strongest Fe XVII lines in order to provide accurate and reliable ratios to compare with theory over the full range of temperatures for which Fe XVII lines are emitted in the corona. This allows us to assess the accuracy of the current theoretical work.

II. DATA

The observations were made by the SOLEX B RAP spectrometer, which is described by Landecker, McKenzie, and Rugge (1979). The spectrometer is equipped with a one arc-minute square multigrid collimator which enables it to isolate part of a single active region for observation. The detector, a channel electron multiplier array, is described in detail by Eng and Landecker (1981). Thirty-seven nonflare spectra were analyzed. Each nonflare spectrum was made by summing several (typically ~ 10) spectral scans. The time between successive scans over a given spectral line was usually 88 s, and 22.3 s were required to scan the wavelength range of primary interest (15.0 - 17.1 Å). For a few of the spectra, the scan rate was twice that described above. In addition, 16 single-scan flare spectra were included in the data sample.

The following lines were used in determining the Fe XVII ratios: $1s^2 2s^2 2p^6\ {}^1S_0 - 2p^5 3d\ {}^1P_1$ (15.01 Å), $2p^6\ {}^1S_0 - 2p^5 3d\ {}^3D_1$ (15.26 Å), $2p^6\ {}^1S_0 - 2p^5 3s\ {}^1P_1$ (16.77 Å), $2p^6\ {}^1S_0 - 2p^5 3s\ {}^3P_1$ (17.05 Å), and $2p^6\ {}^1S_0 - 2p^5 3s\ {}^3P_2$ (17.10 Å). We use the conventional LS coupling nomenclature even though significant mixing occurs between the J=1 levels in the 3s configuration and among the two 3d, J=1 levels already mentioned and the 3d $^3P_1$ level (LN). Figure 1a is a sample nonflare spectrum in the 14-18 Å range with the above lines labeled. We also made use of the

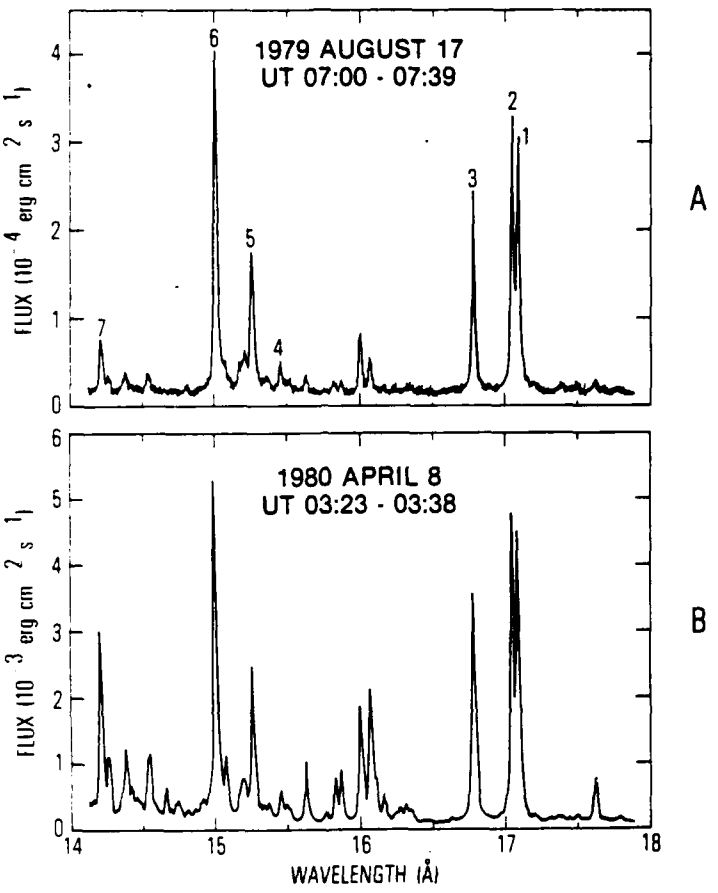

Fig. 1. (a) The X-ray spectrum between 14 and 18 Å from McMath Region 16224 on 1979 August 17, obtained by averaging 14 SOLEX B spectral scans. The following Fe XVII lines are marked: (1) $2p^6\ ^1S_0$ (g) - $2p^5 3s\ ^3P_2$, (2) g - $2p^5 3s\ ^3P_1$, (3) g - $2p^5 3s\ ^1P_1$, (4) g - $2p^5 3d\ ^3P_1$, (5) g - $2p^5 3d\ ^3D_1$, and (6) g - $2p^5 3d\ ^1P_1$. Feature (7) is a blend of Fe XVIII lines: $2p^5\ ^2P_{3/2}$ - $2p^4(^1D)3d\ ^2D_{5/2}$, $^2P_{3/2}$. (b) The spectrum of a solar flare on 1980 April 8, obtained by averaging 5 spectral scans.

feature at 14.20 Å, a blend of Fe XVIII lines, $1s^2 2s^2 2p^5\ ^2P_{3/2}$ - $2p^4(^1D)3d\ ^2D_{5/2}$ and $2p^5\ ^2P_{3/2}$ - $2p^4(^1D)3d\ ^2P_{3/2}$ as a temperature diagnostic. Figure 1b shows the same spectral region for a class M4 flare (Doschek et al. 1981). The figures are plotted in such a way that the flux in a given line may be directly estimated by reading the peak value and subtracting the background, which appears as a continuum. Note that the Fe XVII line fluxes in the flare spectrum are approximately 15 times as strong as those in the nonflare spectrum. Of all the strong lines in the figures, only the O VIII line at 16.01 Å is not an iron line.

In our analysis we obtained the line fluxes by integrating counting-rate spectra over the line profiles and subtracting background, which included a contribution from solar continuum emission. We estimate that systematic line-ratio errors that are associated with the integration procedure are less than 5%. Systematic errors due to uncertainties in the instrument response are estimated to be less than 14% for ratios involving two lines, one near 15 Å and the other near 17 Å. When the lines in a ratio are either both near 15 Å or both near 17 Å, instrumental response uncertainties are negligible. In general, statistical errors are small compared to systematic errors for strong lines such as those of Fe XVII. The $2p^6\ ^1S_0$ - $2p^5 3d\ ^1P_1$ line, at 15.01 Å, lies in a wavelength region which is spectrally complex, and may be contaminated by blended lines, especially in flare spectra.

Phillips et al. (1982) found an unidentified line at 15.039 Å in a high-resolution Solar Maximum Mission (SMM) flare spectrum. Acton (1984) has estimated that this line is about one-eighth as strong as the 15.01 Å line in the SMM flare spectrum. Therefore, overestimation of the 15.01 Å flux by ~ 10% in our flare spectra cannot be ruled out. We believe that contamination by blending is less significant in the nonflare spectra. However, satellite lines emitted following dielectronic recombination to form doubly excited Fe XVI are relatively strong at low temperatures (SRMC). The satellite line transitions are between Fe XVI configurations $2p^5 3dn\ell$ and $2p^6 n\ell$. Our 15.01 Å line fluxes, obtained by integration over the line profiles, include the unresolved satellite lines (those for which $n > 3$). According to SRMC the effect of including these lines is to reduce measured line ratios with the 15.01 Å line in the denominator by 30% at 2.5×10^6 K and by 14% at 5.0×10^6 K.

Loulergue and Nussbaumer (1973, LN) calculated the Fe XVII X-ray line emission. Their calculation took cascade into account and included 51 levels for which $n \leq 4$, where n is the principal quantum number of the outermost electron. The calculated line ratios were compared with the observations available at the time, and the agreement was pronounced reasonable in most cases. The variation in the ratios compiled from different sources (LN) was greater than the variation in the SOLEX data itself. It is likely

that the observed wide variation resulted from unrecognized systematic errors in some of the early measurements.

SRMC have recently recalculated the Fe XVII X-ray spectrum. The major new feature of their calculation is that the process of resonance excitation is taken into account. The process follows the dielectronic capture of a free electron by Fe XVII to form Fe XVI in a doubly excited state. The Fe XVI ion may autoionize to Fe XVII in the ground state, providing the excess energy to the ejected electron, or undergo a radiative transition that leaves it with insufficient energy to autoionize. Resonance excitation takes place when a doubly excited Fe XVI ion with sufficient energy autoionizes to an excited level of Fe XVII. Because $2s^2 2p^5 3s$ is the lowest excited configuration for Fe XVII, its levels are available for resonance excitation at the lowest threshold Fe XVI energy. The result is that the lines with 3s upper levels are strengthened with respect to those with 3d upper levels at low temperatures. Line ratios of the form $I(2p^6\ {}^1S_0 - 2p^5 3s\ {}^xP_y)/I(2p^6\ {}^1S_0 - 2p^5 3d\ {}^1P_1)$ are strongly temperature dependent when $10^6\ K < T < 10^7\ K$, falling off with increasing temperature. In contrast, LN predicted a slow increase in these ratios with increasing temperature. Comparing their results with recent observations, SRMC conclude that Fe XVII lines are formed in active regions predominantly at temperatures of $2\text{-}3 \times 10^6$ K. Our calculations, which use the $2p^6\ {}^1S_0 - 2p^5 3d\ {}^1P_1$ collision

strengths tabulated in Merts *et al.* (1980) and the ionization equilibrium of Jacobs *et al.* (1977), indicate that Fe XVII line formation is inefficient for $T \leq 2.5 \times 10^6$ K. Therefore, the low temperature estimate of SRMC is difficult to reconcile with the common presence in active-region spectra of the lines of Fe XVIII, Mg XI, and even Mg XII, each of which is calculated to be weak for temperatures less than 3×10^6 K.

III. RESULTS

A. 3s/3d LINE RATIOS

The flux ratios involving one 3s upper level and one 3d upper level are of the most potential interest because recent calculations (SMRC) indicate that they have significant temperature sensitivity. In Figure 2, the ($2p^6\ ^1S_0$ - $2p^5 3s\ ^3P_1$)/($2p^6\ ^1S_0$ - $2p^5 3d\ ^1P_1$) energy flux ratio is plotted against the ratio of the Fe XVIII 14.20 Å energy flux to the Fe XVII $2p^6\ ^1S_0$ - $2p^5 3d\ ^1P_1$ (15.01 Å) energy flux. [The notation $R_E(\lambda_1/\lambda_2)$ is used in the figures to represent the ratio of energy flux of a line at λ_1 to that of a second line at λ_2.] The latter ratio is a temperature indicator, and a second horizontal scale gives the temperature T' derived from it. The 14.20 Å and 15.01 Å line fluxes were calculated as functions of temperature, as explained in McKenzie and Landecker (1981), by using collision strengths from Merts et al. (1980) and the ionization equilibrium calculations of Jacobs et al. (1977). It might be argued that the Fe XVII and Fe XVIII emissions come from separate regions, but calculations show that it is only at temperatures above 7×10^6 K that Fe XVIII emission is strong while Fe XVII emission is weak. Only if there is one region for which $T \gtrsim 7 \times 10^6$ K, one for which $T \lesssim 4 \times 10^6$ K, and no significant region for which $4 \times 10^6\ K < T < 7 \times 10^6$ K would the emissions be spatially separated. Therefore, the Fe XVIII/ Fe XVII ratio should provide an approximate

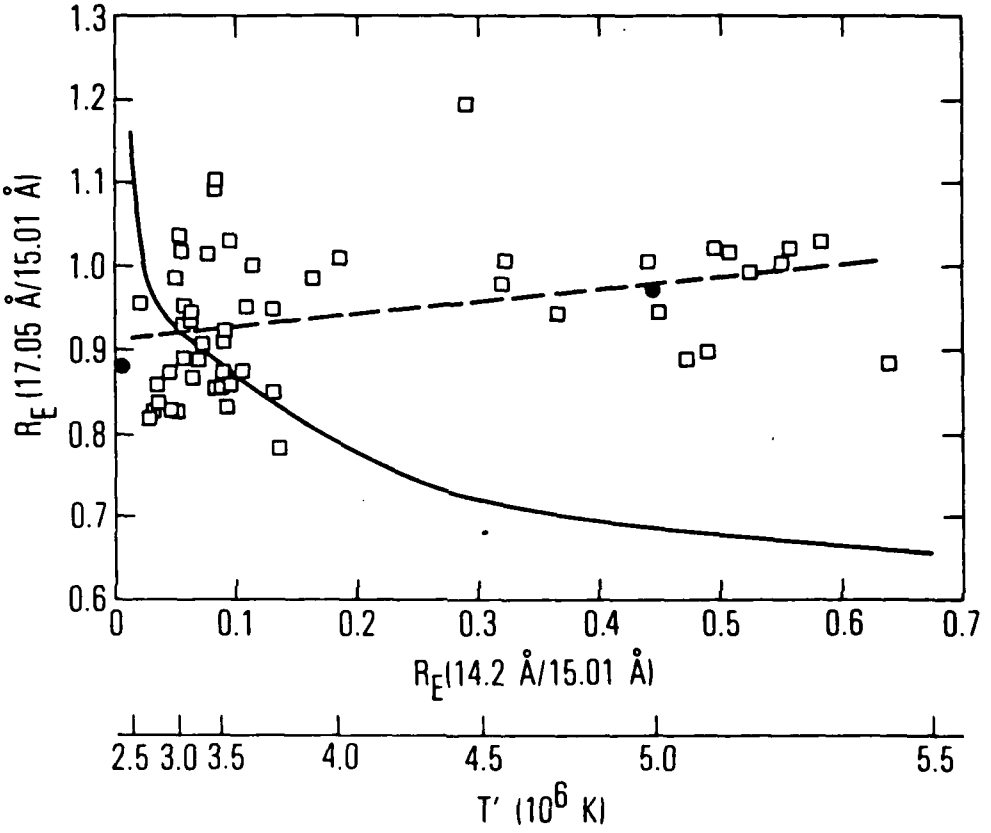

Fig. 2. The energy flux ratio of two Fe XVII lines, ($2p^6\ ^1S_0$ - $2p^5 3s\ ^3P_1$)/($2p^6\ ^1S_0$ - $2p^5 3d\ ^1P_1$), plotted as a function of the energy flux ratio of (Fe XVIII $2p^5\ ^2P_{3/2}$ - $2p^4(^1D)3d\ ^2D_{5/2}$, $^2P_{3/2}$)/(Fe XVII $2p^6\ ^1S_0$ - $2p^5 3d\ ^1P_1$). A second horizontal scale gives the temperature T' deduced from the latter ratio. The solid line gives the theoretical ratio as a function of temperature (SRMC), and the dashed line gives the linear least-squares best fit to the data. The calculations of LN are shown as filled circles.

indicator of the average temperature in the Fe XVII emitting region. The solid curve in Figure 2 shows the line ratio as calculated by SRMC, plotted as a function of the temperature T' inferred from the Fe XVIII/Fe XVII line ratio. The dashed line shows an unweighted linear least-squares fit to the SOLEX data.

The agreement between the observed and calculated flux ratios shown in Figure 2 is poor. The observed ratio increases with increasing temperature; the opposite behavior was predicted by SRMC. The scatter in the measured data is substantial, especially at low temperature. At low temperature, the Fe XVIII counting rates are low and the uncertainties in the Fe XVIII/Fe XVII flux ratios are relatively large. Therefore it would not be unreasonable to conclude that the low-temperature data are scattered, in the horizontal dimension, about the SRMC curve. However, the higher-temperature data cannot be reconciled with the theory. The separation between the theoretical and observational curves is too large to be attributed to instrumental uncertainties, even if possible blending with the 15.01 Å line is taken into account. In fact, correction for any such blending would only result in a larger discrepancy between the observed and predicted line flux ratios. The agreement between the observations in Figure 2 and the calculation of LN is good (see the filled circles in the figure), but this is probably coincidental, since this older calculation was much less

comprehensive than that of SRMC, and the basic atomic parameters used in both calculations were essentially the same. Furthermore, for the other two 3s/3d line ratios, to be presented below, the observations do not agree with the LN calculations. Previous measurements (Parkinson 1975; Walker, Rugge, and Weiss 1974; and Hutcheon, Pye, and Evans 1976) of the ratio under discussion, all of which had poorer counting statistics than the SOLEX measurements, have a wider range than the SOLEX observations and average about 15% lower.

Figures 3 and 4 display the ratios, R_E(16.77 Å/15.01 Å) of the $(2p^6\ {}^1S_0 - 2p^5 3s\ {}^1P_1)/(2p^6\ {}^1S_0 - 2p^5 3d\ {}^1P_1)$ lines and R_E(17.10 Å/15.01 Å) of the $(2p^6\ {}^1S_0 - 2p^5 3s\ {}^3P_2)/(2p^6\ {}^1S_0 - 2p^5 3d\ {}^1P_1)$ lines, respectively, in a manner similar to Figure 2. For the former case, the measured ratios agree fairly well in magnitude with the calculations of SRMC, but the temperature dependence of neither ratio agrees with their calculations. The disagreement is particularly severe for the 3s $^3P_2$/3d $^1P_1$ ratio, for which a relatively strong inverse temperature dependence is predicted, and a weak direct dependence is observed. For all three 3s/3d ratios, the observed temperature dependence is similar to that of LN, but in the last two cases discussed here, the magnitudes of the ratios measured and calculated disagree significantly. For the 3s $^3P_2$/3d $^1P_1$ ratio, previous measurements (Parkinson 1975; Walker, Rugge, and Weiss 1974; and Hutcheon, Pye,

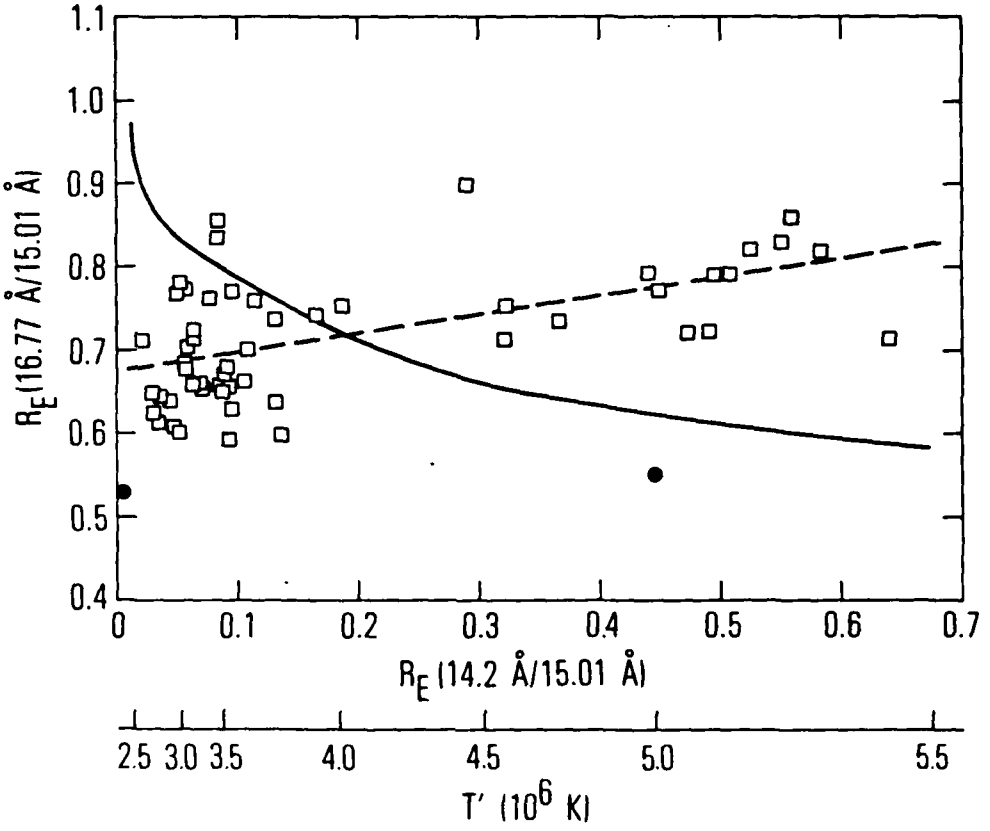

Fig. 3. The energy flux ratio of two Fe XVII lines, ($2p^6\ ^1S_0$ - $2p^5 3s\ ^1P_1$)/($2p^6\ ^1S_0$ - $2p^5 3d\ ^1P_1$), plotted with the same conventions as in Fig. 2.

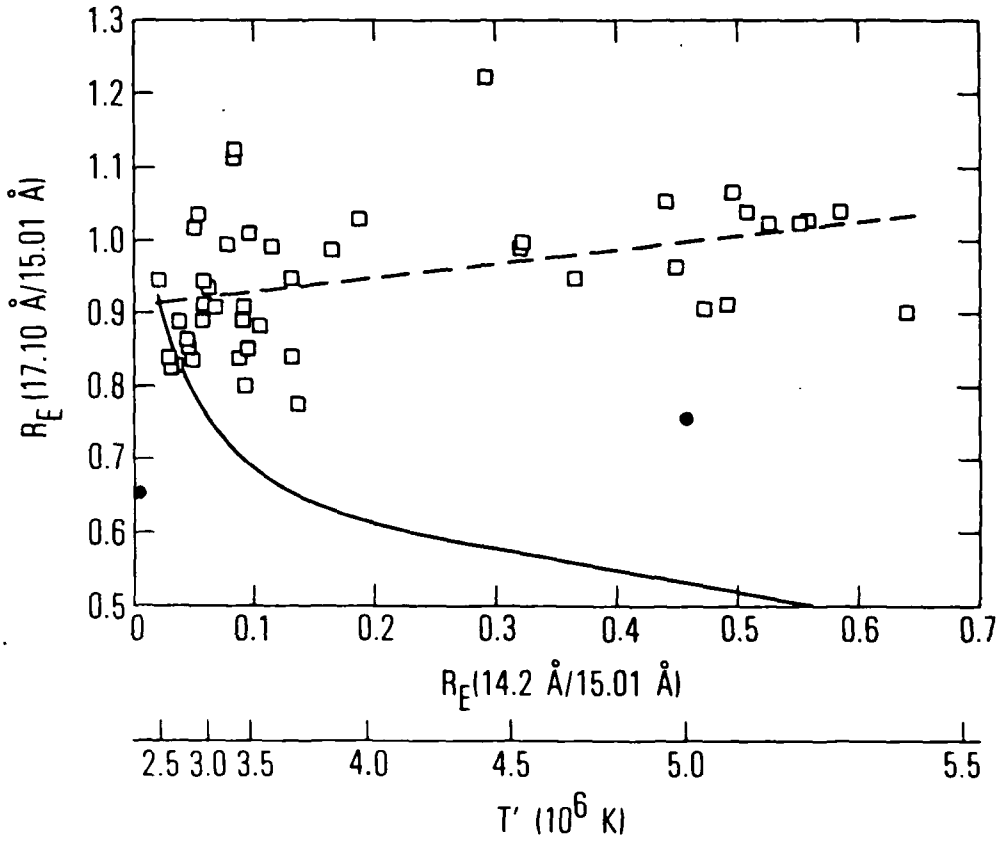

Fig. 4. The energy flux ratio of two Fe XVII lines, ($2p^6\ ^1S_0$ - $2p^5 3s\ ^3P_2$)/($2p^6\ ^1S_0$ - $2p^5 3d\ ^1P_1$), plotted with the same conventions as in Fig. 2.

and Evans 1976) display considerable scatter and average about 15% smaller than the SOLEX values. For the 3s $^1P_1$/3d $^1P_1$ ratio, the SOLEX observations agree well with the previous work cited above.

In summary, the SOLEX observations indicate that the 3s/3d line ratios increase very slowly with increasing electron temperature. The calculations of SRMC predicted a relatively strong inverse temperature relationship for these ratios and kindled hope that the ratios could be used as temperature diagnostics. The disagreement between theory and observation has shown that such use cannot be made of these ratios. Furthermore, the observed weak temperature dependence probably means that the line ratios will not be useful as temperature diagnostics in the future either, because experimental and theoretical accuracy would both have to improve dramatically.

B. 3s/3s LINE RATIOS

Figure 5 shows the ($2p^6\ ^1S_0$ - $2p^5 3s\ ^3P_1$)/($2p^6\ ^1S_0$ - $2p^5 3s\ ^3P_2$) line ratio, R_E(17.05 Å/17.10 Å), plotted as in Figure 2. The data show a weak temperature dependence and very little scatter. Neither the LN calculation nor that of SRMC agrees with the observations. Previous observations (Parkinson 1975; Walker, Rugge, and Weiss 1974; and Hutcheon, Pye, and Evans 1976) of this ratio, which were limited by counting statistics, have a much wider range than the SOLEX observations. This is true even for different observations with the same instrument. The average of

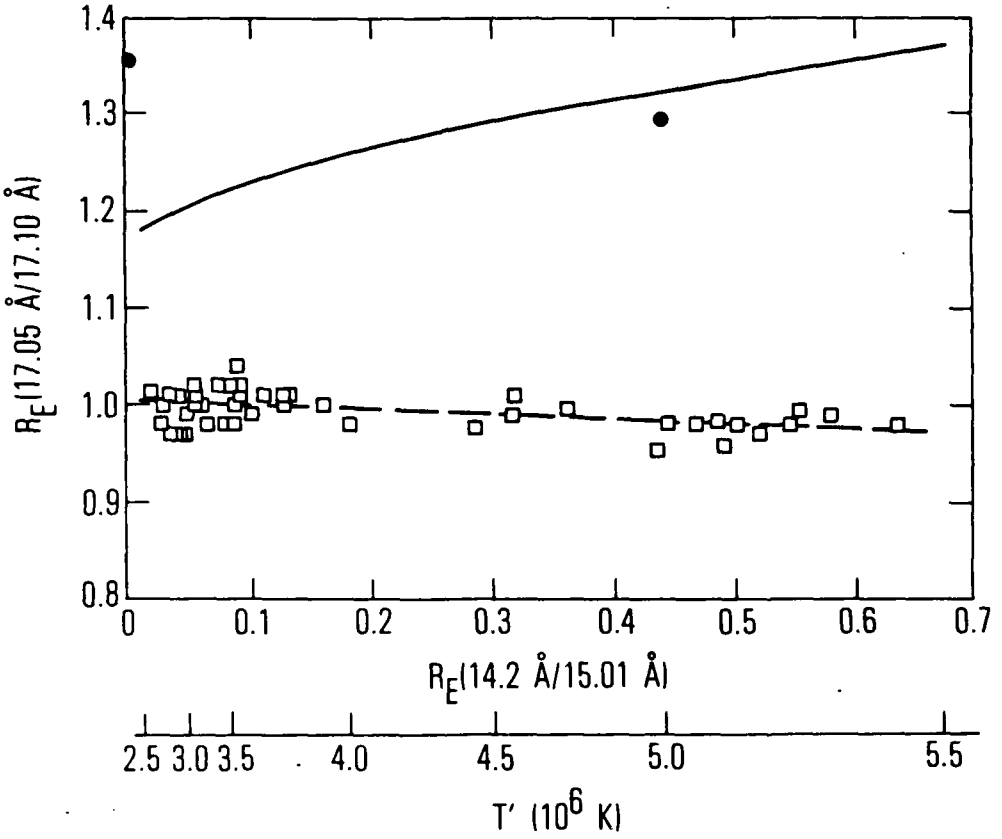

Fig. 5. The energy flux ratio of two Fe XVII lines ($2p^6\ ^1S_0$ - $2p^5 3s\ ^3P_1$)/($2p^6\ ^1S_0$ - $2p^5 3s\ ^3P_2$), plotted with the same conventions as in Fig. 2. Note that the vertical scatter in the data is much less than that for the 3s/3d ratios in Figs. 2 through 4.

these measurements agrees reasonably well with the SOLEX results. For this one ratio we can compare our measurements with those of the Solar Maximum Mission Flat Crystal Spectrometer experiment. Phillips et al. (1982) report values of 1.07 and 1.00 for observations of two solar flares. The agreement with SOLEX is good.

Figure 6 is a plot of the $(2p^6\ ^1S_0 - 2p^5 3s\ ^1P_1)/(2p^6\ ^1S_0 - 2p^5 3s\ ^3P_1)$ energy flux ratio, R_E(16.77 Å/17.05 Å). Although the measured ratios are closer to the SRMC calculation than most of the other ratios discussed so far, the data cannot be said to agree with the theory. The experimental uncertainties are small. Previous observations show a wide range of values, as they did for the other ratios we have discussed, and on the average are somewhat higher than the SOLEX average.

C. 3d/3d LINE RATIOS

Figure 7 shows the $(2p^6\ ^1S_0 - 2p^5 3d\ ^3D_1)/(2p^6\ ^1S_0 - 2p^5 3d\ ^1P_1)$ energy flux ratio. The temperature dependence of the measured ratios is in agreement with the calculations. This is not surprising since collisional excitation dominates the formation of both lines (SRMC), and the calculation is therefore relatively simple. The observed ratios are substantially larger than the calculated ones but agree well with previous observations (Parkinson 1975; Walker, Rugge, and Weiss 1974; and Hutcheon, Pye, and Evans 1976). As has been the case for all of the ratios

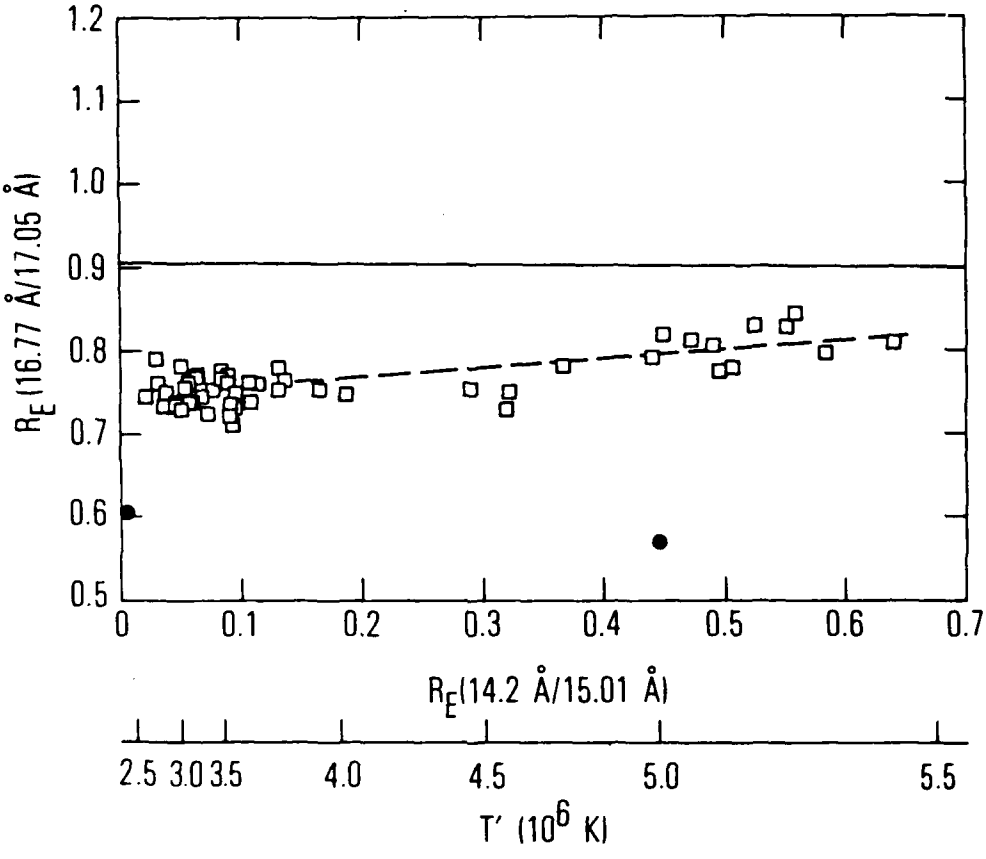

Fig. 6. The energy flux ratio of two Fe XVII lines, ($2p^6\ ^1S_0 - 2p^5 3s\ ^1P_1$)/($2p^6\ ^1S_0 - 2p^5 3s\ ^3P_1$), plotted with the same conventions as in Fig. 2. Again, ratios not involving the 15.01 Å line show significantly less scatter than those that include this line.

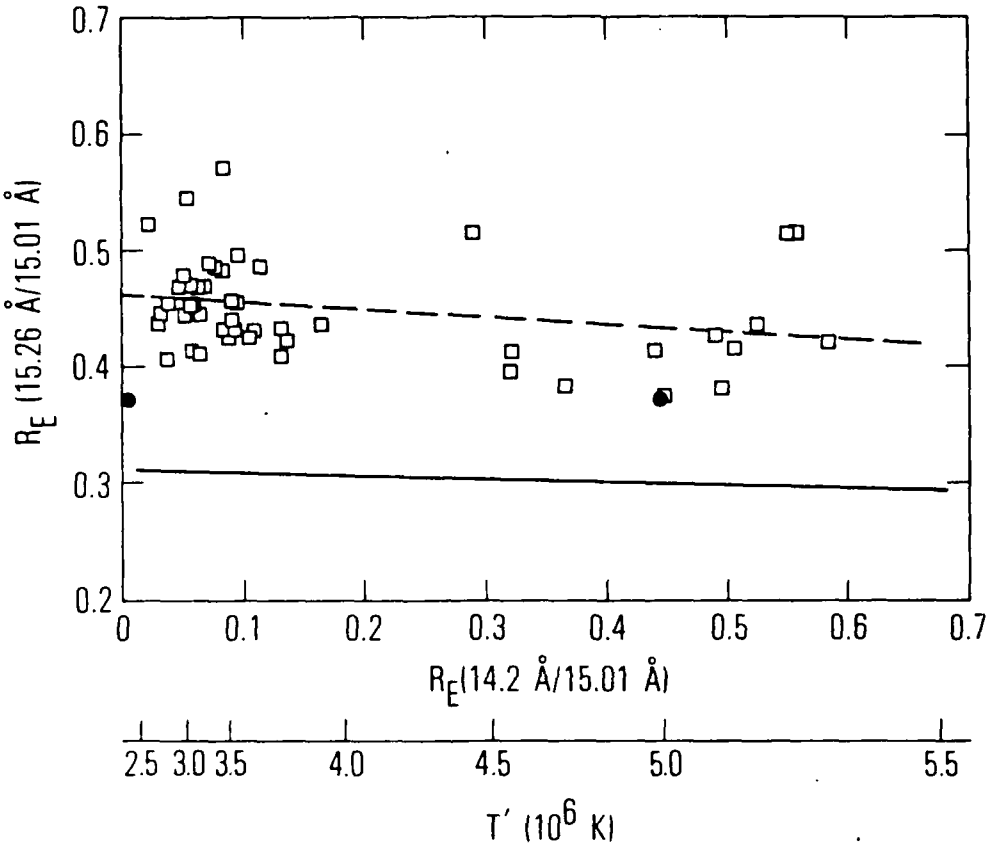

Fig. 7. The energy flux ratio of two Fe XVII lines, ($2p^6\ ^1S_0$ - $2p^5 3d\ ^3D_1$)/($2p^6\ ^1S_0$ - $2p^5 3d\ ^1P_1$), plotted with the same conventions as in Fig. 2.

involving the $2p^6\ ^1S_0 - 2p^5 3d\ ^1P_1$ resonance transition, the data show considerable scatter.

The $(2p^6\ ^1S_0 - 2p^5 3d\ ^3P_1)/(2p^6\ ^1S_0 - 2p^5 3d\ ^1P_1)$ line ratio, R_E(15.45 Å/15.01 Å), is also of potential interest. SRMC predict a relatively strong temperature dependence, with the energy ratio decreasing from 0.058 at 2.5×10^6 K to 0.045 at 5×10^6 K. In contrast LN predict a weaker temperature dependence with energy ratios of 0.11 at 2×10^6 K and 0.13 at 5×10^6 K. The $^3P_1$ line, at 15.45 Å, is weak and lies in a spectral region where the background is difficult to determine. Therefore we have not made a detailed study of the SOLEX spectra for this line. However, we have evaluated the above-mentioned ratio for several nonflaring and flaring spectra, obtaining values between 0.07 and 0.10 with uncertainties large enough (0.01 to 0.02) to prevent us from establishing a clear temperature dependence.

D. RESONANCE SCATTERING

The phenomenon of resonance scattering may partially account for the large variance in the ratios involving the $2p^6\ ^1S_0 - 2p^5 3d\ ^1P_1$ line. In this process, a resonance line photon is absorbed by an ion in the ground state. The excited ion then emits a resonance line photon at the same wavelength, which, in general, propagates in a new direction. The effect of this absorption and re-emission cannot be distinguished from scattering. Depending on the source geometry, the result may be

either an enhancement or a diminution of the resonance line flux measured by a remote detector.

Chandrasekhar (1960) has treated resonance line scattering. For $J = 1 \rightarrow 0$ resonance transitions, such as the one under consideration, the Stokes parameters change as they do for Rayleigh scattering. Knowing this dependence, one can calculate the line flux emerging from a region of known geometry. One simple case obtains when significant resonance absorption takes place between the source and the emitting region. For example, the O VII $1s^2\ ^1S_0 - 1s2p\ ^1P_1$ resonance line is produced in solar active regions at $T \approx 2 \times 10^6$ K, but the O VII ion accounts for at least half of the oxygen present in the entire coronal plasma for which 3×10^5 K $< T < 2 \times 10^6$ K (Jacobs et al. 1978). The resonance line radiation therefore is absorbed in the relatively cool quiet corona, which is a weak emission source of the radiation. The degree of resonance scattering for O VII has been shown to be well correlated with calculated path lengths through a simple model quiet corona (McKenzie and Landecker 1982). For Fe XVII such scattering (without strong emission) would require an extensive intervening region at a temperature of $2 - 2.5 \times 10^6$ K. There is no independent evidence for the existence of such a region. For example, no SOLEX spectrum shows both strong O VII emission and weak Fe XVII emission.

In the solar corona, the effects of resonance scattering are

most apparent in the spectra of the helium-like ions such as O VII and Ne IX. To see this, one examines the ratio G, defined by

$$G = \frac{I(1s^2\ {}^1S_0 - 1s2p\ {}^3P) + I(1s^2\ {}^1S_0 - 1s2s\ {}^3S_1)}{I(1s^2\ {}^1S_0 - 1s2p\ {}^1P_1)} \qquad (1)$$

where I stands for line intensity. In this ratio, the resonance line, in the denominator, is affected by resonance scattering, while the intercombination (^3P) and forbidden (^3S) lines are not. Therefore, if resonance line photons are scattered out of the line of sight, G increases. Since the lines of Ne IX are emitted in the same temperature range as those of Fe XVII, one might expect the effects of resonance scattering to be similar for the two ions. However, Ne IX accounts for more than half of the neon present in the quiet corona ($T \approx 1.5 \times 10^6$ K) where Fe XVII is relatively scarce (Jacobs et al. 1977). Therefore resonance scattering in the quiet corona should be important for Ne IX, but not for Fe XVII. In this connection, McKenzie and Landecker (1982) have shown that G for Ne IX is positively correlated with the integral of the electron density n_e along the line of sight between the detector and the solar active region under observation. Furthermore, G has a temperature dependence that, while weak (Pradhan, 1982), is opposite to the even weaker temperature dependence observed for the Fe XVII 3s/3d $^1P_1$ line

ratios. Taking these facts into account, we expect a weak correlation between G for Ne IX and such Fe XVII line ratios as R_E(16.77 Å/15.01 Å). When this comparison was made for several SOLEX spectra, we found a weak positive correlation between the ratios, but the data scatter was so large that no definitive conclusion could be drawn. Observations of McMath Region 16161 on the west limb on 1979 July 23-24 are particularly interesting. This region accounts for the two highest Fe XVII 3s/3d line ratios in both Figures 2 and 3. For the spectrum from which the lower-temperature points were drawn, G(Ne IX) = 1.20 and G(O VII) = 2.69. For the higher-temperature spectrum, G(Ne IX) cannot be determined reliably because of possible blending between the Ne IX lines and Fe XIX lines, but G(O VII) = 2.25. These very large G ratios are to be compared with normal values, in the absence of resonance scattering, of 1.00 for O VII and 0.80 for Ne IX (McKenzie and Landecker 1982). The McMath 16161 values are the highest we have ever observed with the SOLEX spectrometers for their respective ions and are indicative of very strong resonance scattering. The corresponding high Fe XVII 3s/3d line ratios for these two spectra almost certainly can be attributed to resonance scattering of the $2p^6\ {}^1S_0 - 2p^5 3d\ {}^1P_1$ line.

The resonance scattering absorption coefficient at line center is given by Acton (1978) for J = 1 → 0 transitions (adapted for Fe XVII):

$$\kappa_0 = 9.31 \times 10^{-18} f_{\ell u} A_{26} a_{17} n_e \lambda \left(\frac{M}{T_6}\right)^{1/2} \text{ cm}^{-1} \qquad (9)$$

where $f_{\ell u}$ is the absorption oscillator strength, A_{26} is the iron abundance, a_{17} is the fraction of the iron ions that are Fe XVII, λ is the wavelength in Å, M is the mass in atomic mass units, n_e is the electron density, and T_6 is the temperature in units of 10^6 K. For the Fe XVII resonance line under consideration, $f_{\ell u} = 2.22$ (Mori, Otsuka, and Kato 1979) and $\kappa_0 = 6.2 \times 10^{-20} n_e$ for $T = 2.5 \times 10^6$ K, a typical active-region temperature. To derive this result, we set $A_{26} = 5.25 \times 10^{-5}$ (Withbroe 1976) and used the ionization equilibrium calculations of Jacobs et al. (1977). Setting $n_e \ell = 5 \times 10^{18}$ cm^{-2} (McKenzie and Landecker 1982), where ℓ is a characteristic length for an active region, we find that the optical depth for resonance scattering at line center, $\tau_0 \approx 0.3$. For the 3s lines, τ_0 is $\lesssim 0.05$ times this value; hence, for them, resonance scattering is negligible. As we noted above, the manner in which resonance scattering affects the remotely detected line flux depends on the detailed geometry of both the emitting regions and the regions through which the radiation propagates. The estimated τ_0 indicates that resonance scattering can explain the relatively wide variation in the 3s/3d line ratios in Figures 2-4. The geometry of McMath Region 16161 when it was on the limb was apparently favorable for scattering resonance line photons out of

the beam from the lower corona to the observer.

The 3d $^3D_1$/3d $^1P_1$ line ratio, R_E(15.26 Å/15.01 Å), like the 3s/3d $^1P_1$ ratios, varies widely at low temperatures. Resonance scattering could account for this variation as well. For the $^3D_1$ line, τ_0 from equation (2) is 0.24 times τ_0 for the $^1P_1$ line (Mori et al. 1979; LN). Therefore the effect of resonance scattering on the ratio of these two lines is only slightly moderated compared to its effect on the 3s/3d ratios.

IV. SUMMARY

We have analyzed 53 Fe XVII solar X-ray spectra that cover a very wide range of solar activity, including observations of 10 flares at various stages of development. The data comprise the most complete set of spectra in the 15-17 Å wavelength range and have excellent spatial and spectral resolution and counting statistics. The spectra were compared, as a function of temperature, with recent calculations (LN, SRMC). For the purposes of this comparison, a ratio of Fe XVIII and Fe XVII line fluxes was used as a temperature indicator.

We have drawn the general conclusion that the measured Fe XVII line ratios do not agree with the calculations. Those ratios involving one line with a 3s upper level ($\lambda \approx 17$ Å) and the other with a 3d upper level ($\lambda \approx 15$ Å) were predicted to have a significant temperature dependence (SRMC), decreasing with increasing temperature. The observations cannot be reconciled with this prediction. The observed temperature dependence is so weak that it is unlikely that, even with improved theoretical understanding, these ratios will be useful as temperature diagnostics in the foreseeable future. None of the line ratios involving only lines with 3s upper levels agrees satisfactorily with theory, either in the form of the temperature dependence or in the absolute values. The 3s levels are populated primarily by cascade from higher levels (LN, SRMC) and by resonance excitation

(SRMC), while the 3d levels are populated predominantly by direct collisional excitation. Because of this, the strengths of the 3s transitions to the ground state are relatively difficult to calculate. The data indicate that more theoretical work is needed in this area. In contrast, theory accurately predicted the (very weak) temperature dependence of the 3d $^3D_1$/3d $^1P_1$ ratio, R_E(15.26 Å/15.01 Å), although the absolute values of the observed ratios were substantially higher than the predictions.

Simple calculations indicate that resonance scattering of the $2p^6\ ^1S_0 - 2p^5 3d\ ^1P_1$ radiation should be significant, and observations appear to bear out this prediction. The wide variations in the ratios involving the 3d $^1P_1$ line can be accounted for by this process. The observations of McMath Region 16161 on the west limb clearly show resonance scattering effects. However, the influence of resonance scattering on the observed 3d $^1P_1$ line flux depends on the complex geometry of the active region being observed. Therefore the observation of resonance scattering effects has limited diagnostic potential.

REFERENCES

Acton, L. W. 1978, Ap. J., 225, 1069.

_____. 1984, private communication.

Chandrasekhar, S. 1960, Radiative Transfer (New York: Dover), 50-53.

Doschek, G. A., Feldman, U., Landecker, P. B., and McKenzie, D. L. 1981, Ap. J., 249, 372.

Eng, W., and Landecker, P. B. 1981, Nucl. Inst. Meth., 190, 149.

Hutcheon, R. J., Pye, J. P., and Evans, K. D. 1976, M.N.R.A.S., 175, 489.

Jacobs, V. L., Davis, J., Kepple, P. C., and Blaha, M. 1977, Ap. J., 211, 605.

Jacobs, V. L., Davis, J., Rogerson, J. E., and Blaha, M. 1978, J. Quant. Spectrosc. Rad. Transf., 19, 591.

Jordan, C. 1969, M.N.R.A.S., 142, 501.

Landecker, P. B., McKenzie, D. L., and Rugge, H. R. 1979, Proc. Soc. Photo-Opt. Instrum. Eng., 184, 285.

Loulergue, M., and Nussbaumer, H. 1973, Astr. Ap., 24, 209.

Loulergue, M., and Nussbaumer, H. 1975, Astr. Ap., 45, 125 (LN).

McKenzie, D. L., and Landecker, P. B. 1981, Ap. J., 248, 1117.

_____. 1982, Ap. J., 259, 372.

McKenzie, D. L., Landecker, P. B., Broussard, R. M., Rugge, H. R., Young, R. M., Feldman, U., and Doschek, G. A. 1980, Ap. J., 241, 409.

Merts, A. L., Mann, J. B., Robb, W. D., and Magee, N. H., Jr. 1980, Los Alamos Scientific Laboratory LA-8267-MS.

Mori, K., Otsuka, M., and Kato, T. 1979, Atomic Data and Nucl. Data Tables, 23, 195.

Parkinson, J. H. 1973, Astr. Ap., 24, 215.

Parkinson, J. H. 1975, Solar Phys., 42, 183.

Phillips, K. J. H. et al. 1982, Ap. J., 256, 774.

Pradhan, A. K. 1982, Ap. J., 263, 477.

Smith, B. W., Raymond, J. C., Mann, J. B., and Cowan, R. D. 1984, Los Alamos National Laboratory preprint LA-UR-84-1355.

Walker, A. B. C., Jr., Rugge, H. R., and Weiss, K. 1974, Ap. J., 194, 471.

Withbroe, G. L. 1976, Center for Astrophysics Preprint No. 524.

LABORATORY OPERATIONS

The Laboratory Operations of The Aerospace Corporation is conducting experimental and theoretical investigations necessary for the evaluation and application of scientific advances to new military space systems. Versatility and flexibility have been developed to a high degree by the laboratory personnel in dealing with the many problems encountered in the nation's rapidly developing space systems. Expertise in the latest scientific developments is vital to the accomplishment of tasks related to these problems. The laboratories that contribute to this research are:

Aerophysics Laboratory: Launch vehicle and reentry fluid mechanics, heat transfer and flight dynamics; chemical and electric propulsion, propellant chemistry, environmental hazards, trace detection; spacecraft structural mechanics, contamination, thermal and structural control; high temperature thermomechanics, gas kinetics and radiation; cw and pulsed laser development including chemical kinetics, spectroscopy, optical resonators, beam control, atmospheric propagation, laser effects and countermeasures.

Chemistry and Physics Laboratory: Atmospheric chemical reactions, atmospheric optics, light scattering, state-specific chemical reactions and radiation transport in rocket plumes, applied laser spectroscopy, laser chemistry, laser optoelectronics, solar cell physics, battery electrochemistry, space vacuum and radiation effects on materials, lubrication and surface phenomena, thermionic emission, photosensitive materials and detectors, atomic frequency standards, and environmental chemistry.

Computer Science Laboratory: Program verification, program translation, performance-sensitive system design, distributed architectures for spaceborne computers, fault-tolerant computer systems, artificial intelligence and microelectronics applications.

Electronics Research Laboratory: Microelectronics, GaAs low noise and power devices, semiconductor lasers, electromagnetic and optical propagation phenomena, quantum electronics, laser communications, lidar, and electro-optics; communication sciences, applied electronics, semiconductor crystal and device physics, radiometric imaging; millimeter wave, microwave technology, and RF systems research.

Materials Sciences Laboratory: Development of new materials: metal matrix composites, polymers, and new forms of carbon; nondestructive evaluation, component failure analysis and reliability; fracture mechanics and stress corrosion; analysis and evaluation of materials at cryogenic and elevated temperatures as well as in space and enemy-induced environments.

Space Sciences Laboratory: Magnetospheric, auroral and cosmic ray physics, wave-particle interactions, magnetospheric plasma waves; atmospheric and ionospheric physics, density and composition of the upper atmosphere, remote sensing using atmospheric radiation; solar physics, infrared astronomy, infrared signature analysis; effects of solar activity, magnetic storms and nuclear explosions on the earth's atmosphere, ionosphere and magnetosphere; effects of electromagnetic and particulate radiations on space systems; space instrumentation.

. . .

END

FILMED

1-86

DTIC